Honey bee hairs and pollenkitt are essential for pollen capture and removal

IOP Publishing Bioinspir. Biomim. 12 (2017) 026015 https://doi.org/10.1088/1748-3190/aa5c6e

Bioinspiration & Biomimetics

PAPER

RECEIVED
30 August 2016

REVISED
6 December 2016

ACCEPTED FOR PUBLICATION
26 January 2017

PUBLISHED
23 March 2017

Honey bee hairs and pollenkitt are essential for pollen capture and removal

Guillermo J Amador[1], Marguerite Matherne[1], D'Andre Waller[1], Megha Mathews[1], Stanislav N Gorb[3] and David L Hu[1,2]

[1] School of Mechanical Engineering, Georgia Institute of Technology, Atlanta, GA, United States of America
[2] School of Biology, Georgia Institute of Technology, Atlanta, GA, United States of America
[3] Department of Functional Morphology and Biomechanics, Zoological Institute, Kiel University, Christian-Albrechts-Platz, Kiel, Germany

E-mail: hu@me.gatech.edu

Keywords: Apis mellifera, evolution, cleaning, grooming, adhesion

Supplementary material for this article is available online

Abstract

While insect grooming has been observed and documented for over one hundred years, we present the first quantitative analysis of this highly dynamic process. Pollinating insects, like honey bees, purposely cover themselves with millions of pollen particles that, if left ungroomed, would make sensing and controlled flight difficult. How do they get clean? We show that the hairs on insect eyes are tuned to the pollen they collect; namely, the hairs are spaced so that they suspend pollen above the body for easy removal by the forelegs. In turn, hair spacing on the foreleg dictates the leg's ability to store the pollen removed during each swipe. In tests with wax-covered honey bees, we show that hairy forelegs are necessary for pollen removal. Moreover, the viscous fluid found on the surface of pollen grains, or pollenkitt, greatly enhances adhesion. We find that bees accumulate twice as much pollen if pollenkitt is present. This study may help further understand pollination, as well as inform designs for mechanically-sensitive functional surfaces with micro- and nano-structures that are easier to keep clean.

1. Introduction

The Cretaceous and Paleogene Periods (140 to 23 million years ago) brought about great diversification of flowering plants and pollinating insects. Between their first arrival in the early Cretaceous Period to the Paleogene Period, flowering plants evolved from small, apetalous flowers, to the great number of modern flowering plant species, like rosids and asterids [1]. Along with the increasing complexity of flowering plants, flower-visiting insects, of the orders Coleoptera, Diptera, Lepidoptera, and Hymenoptera, flourished. Flowering plants offered insects sweet nectar in exchange for targeted dispersal of their micrometer-scale pollen grains. The ongoing success of this mutualistic relationship is dictated by the interaction between insects and pollen grains, in both collection and removal.

While there have been many observational studies of the grooming behaviors in various insect species [2–11], quantitative analyses of the cleaning process are only recent [12, 13]. The motor organization governing the grooming sequence of fruit flies was determined through genetic manipulation of neural circuitry [12]. Additionally, scanning electron microscopy and simulations of grooming actions were used to determine the grooming efficiency and functional hierarchy of the antennal cleaner of ants [13].

It is known that pollinators usually rely on a vast variety of hairs in collecting, retaining, manipulating, and removing pollen grains [3–5, 8, 9]. In this study, we demonstrate the specialization of insect hairs for pollination, namely for facilitating the removal of accumulated pollen particles. Our model organism for this study is the honey bee *Apis mellifera*, shown in figure 1(a). It covers its body with pollen particles and works meticulously to transfer them to its hindlegs in order to transport them back to the hive. A typical foraging worker honey bee accumulates up to 30% of its body weight in pollen when it visits flowers [14]. The body of a honey bee, as well as other bee species, is covered by millions of hairs, onto which pollen accumulates [15].

In this study, we also demonstrate the importance of the viscous fluid on the surface of pollen grains, or pollenkitt. Previous works have shown that this fluid

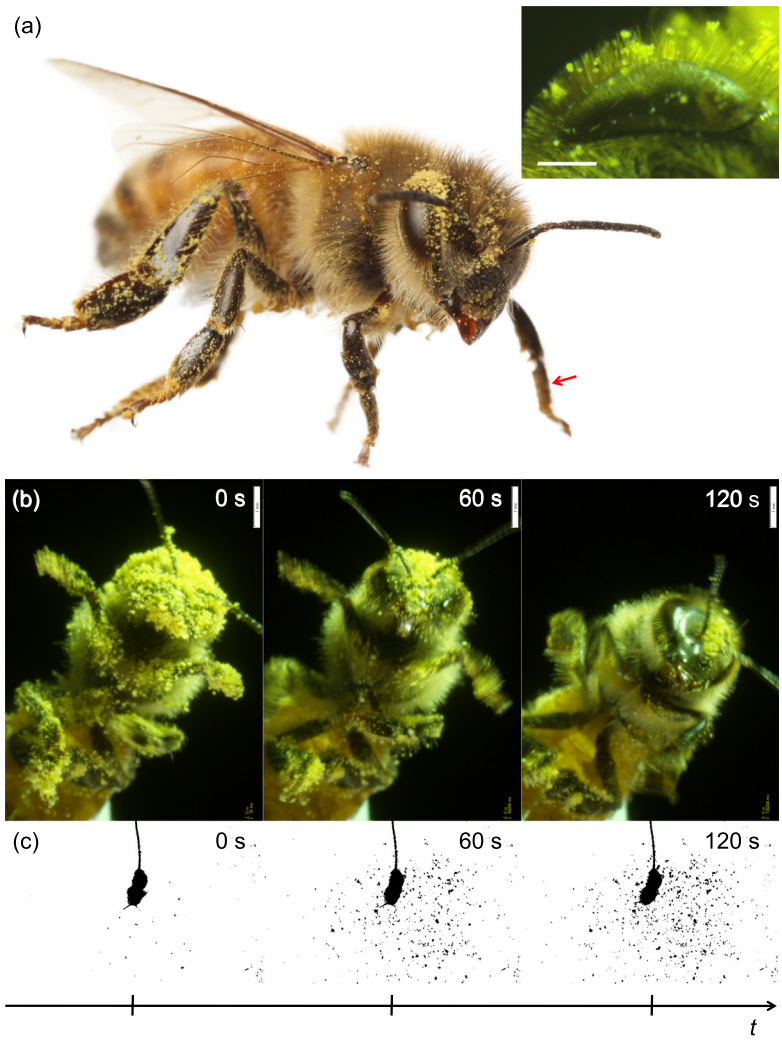

Figure 1. A honey bee *Apis mellifera* grooming itself. (a) A honey bee covered with commercial pollen. The small red arrow denotes the basitarsal segment that is used for grooming the compound eye. Inset shows the compound eye with commercial pollen particles. Scale bar denotes 0.5 mm. (b) Time-lapse photo sequence of a honey bee cleaning its eyes. (c) Time-lapse photo sequence of the pollen removed during grooming.

enhances adhesion by factors of 3–6 [16]. However, their investigation was limited to synthetic substrates. The effects on biological substrates, like insect hair or cuticle, has yet to be explored.

2. Materials and methods

2.1. Observation of pollen removal performance *in situ*

In figure 2(a), we show a schematic of our experimental setup. A live tethered honey bee is coated in pollen and placed underneath a uniform backlight and above an optically transparent glass dish. Honey bees are tethered by attaching a thin wire dorsally to their abdomen with UV curable adhesive (Loctite 4311). The uniform backlight is composed of an acrylic box with aluminum foil lining the inner walls, a 65-watt compact fluorescent light bulb, and a slightly opaque, light-diffusing plate. A camcorder (camcorder *1*, Sony Handycam HDR-XR200) is placed below the dish to observe the pollen falling from the bee and onto the dish. Because of the uniform backlight, the camcorder captures silhouettes of the pollen particles collecting onto the glass dish. Supplementary video 1 (stacks.iop.org/BB/12/026015/mmedia) shows an examples of a video obtained from this perspective. For every second of video, we extract an image and use the MATLAB image analysis toolbox to convert them into black and white images. By supplying a grey tone threshold (between 0 and 1, where 0 is black and 1 is white), we obtain images where each pixel is either black or white. We count the number of black pixels and subtract the value obtained for the initial image at zero seconds to quantify the number of pollen particles removed.

We also implement a second camcorder (camcorder *2*) to film the grooming honey bee from the side and determine how many swipes are required to adequately clean the eyes, as well as the frequency and duration of the swipes. Supplementary video 2 shows an examples of a video obtained from this perspective.

In our experiments we use two different types of pollen particles, one that is commercially available (Stakich Organic Bee Pollen), and dandelion (*Taraxacum officinale*) pollen. The commercial

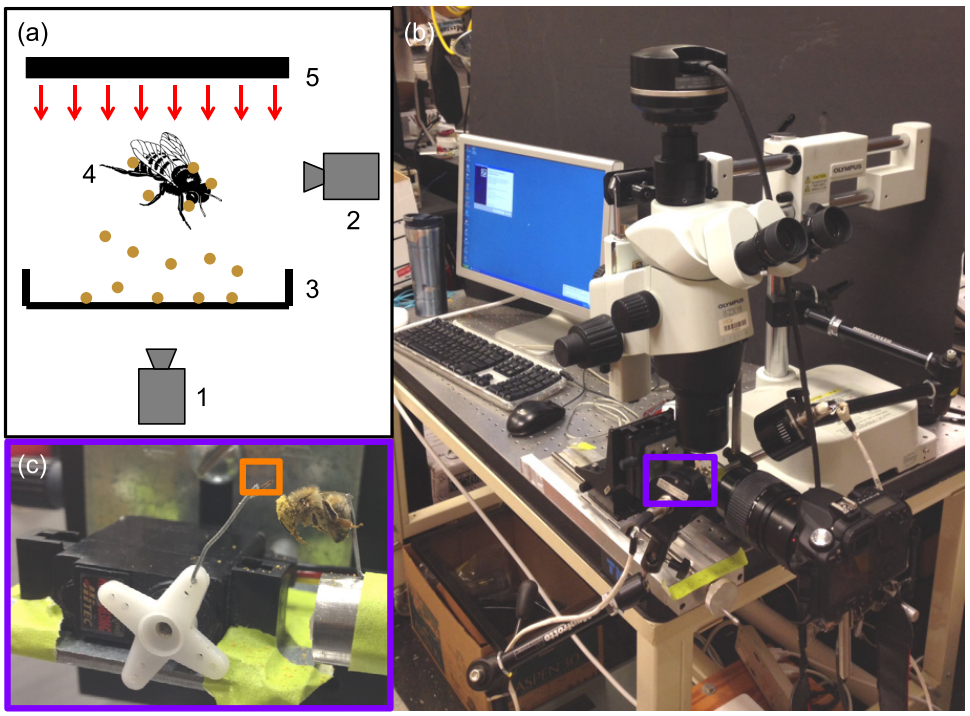

Figure 2. Observing pollen removal during grooming and simulating honey bee eye cleaning. (a) Schematic of the experimental setup using two digital camcorders, denoted by (1) and (2), (3) optically transparent glass dish, (4) live tethered honey bee covered in pollen, and (5) uniform backlight. (b) Picture of experimental setup for replicating honey bee eye cleaning motions using a severed leg attached to a servomotor. (c) Servomotor with leg and the honey bee that the leg swipes across.

pollen particles used are, on average, spherical with diameters of 30 μm, as shown in the scanning electron micrographs in the first column of figures 3(a) and (b). This pollen is collected using pollen traps in northern Asia and may contain pollen from various plants, as well as other biological matter, like sugars from nectar [17].

The fresh dandelion pollen is obtained from Greer Laboratories (Lenoir, NC) and stored at 0 °C. Because it is naturally sourced directly from plants, the pollen has a thin, viscous layer of fluid called pollenkitt [18]. This sticky fluid attracts pollinating insects to the pollen grains through odor and may provide an extra adhesive force so the grains remain attached to the insect. Like the commercial pollen, the natural pollen particles are also roughly spherical with diameters of 25 μm, as shown in the second column of figures 3(a) and (b).

To test the effect of pollenkitt on honey bee grooming, we wash the pollen to remove the sticky fluid. The pollenkitt was removed by washing 1 gram of pollen in 10 ml of a 3:1 mixture of chloroform and methanol, a solvent for pollenkitt but not for the exine of the pollen grain, as described elsewhere [16]. The mixture was spun in a centrifuge at 3000 rpm for 10 min. The pollen and excess liquid were separated by pouring the mixture over filter paper in a glass funnel and drained into a glass beaker. The pollen was then rinsed with 10 ml of ethanol and allowed to dry for approximately 24 h before being used. The washed dandelion pollen is shown in the third column of figures 3(a) and (b).

2.2. Measuring bristle and hair geometries

We measure the bristle lengths L_i and spacings S_i of insects. Here, $i = 0$ denotes the insect forelegs, and $i = 1$ denotes the insect compound eyes. For measuring, we use a scanning electron microscope (LEO 1530 and Phenom G2 Pro) and digitally measure the hair geometries using an open source software (Tracker by Douglas Brown), or measure from other SEM images in the literature [19–25] (see figures 5(a) and table S1). In total, we measure 10 insects (including honey bees).

2.3. High-speed videography

To carefully observe the mechanics of individual grooming behaviors, we use high speed videography. Supplementary video 3 shows two typical swipes of the foreleg across the eye.

The basitarsal kinematics during grooming are determined by tracking the motion of the pollen brush across the eye. To do so, we mark the foreleg of live honey bees ($N = 2$) with two white dots of paint at the proximal and distal extents of the basitarsus and track their motion. Using a high speed camera (Phantom v210) viewing through an optical microscope (Olympus SZX16) we film honey bee eye cleaning motions at a frame rate of 1000 frames per second. Both

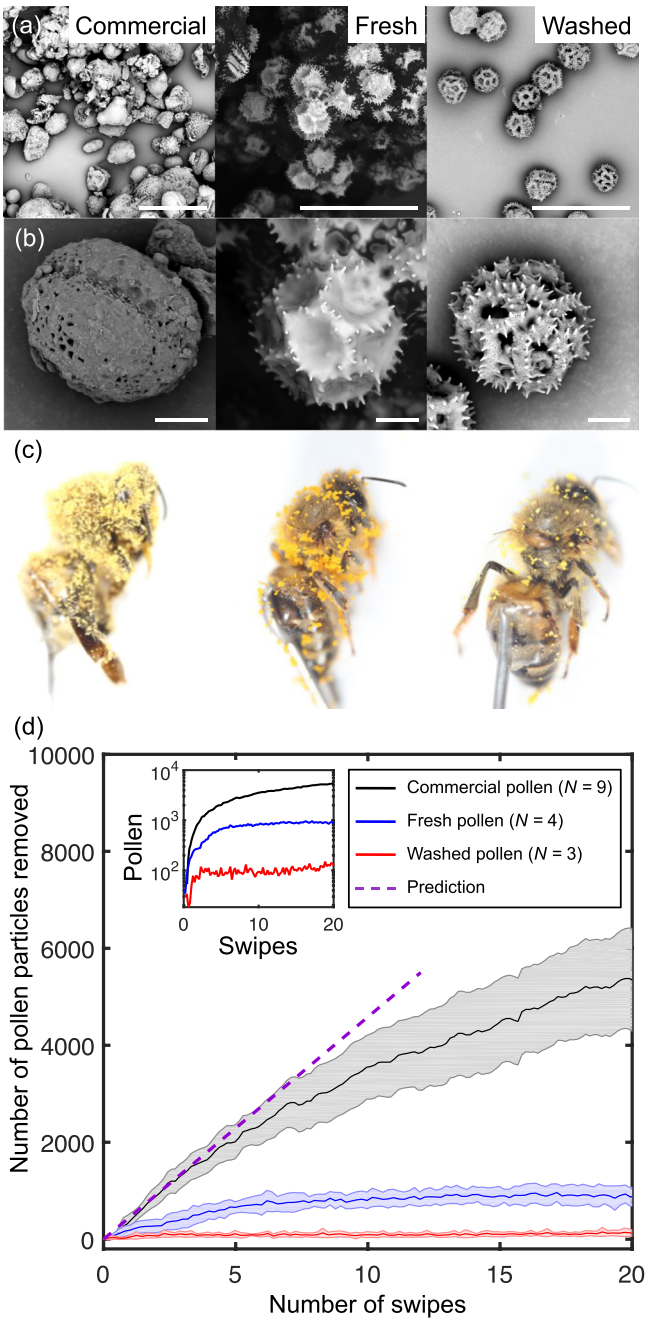

Figure 3. Grooming performance. ((a)–(b)) Scanning electron micrographs of commercial pollen (first column), and dandelion (*Taraxacum officinale*) pollen with (second column) and without (third column) pollenkitt. Scale bars represent (a) 100 μm and (b) 10 μm. (c) Bees covered in commercial pollen (first column), and dandelion pollen with (second column) and without (third column) pollenkitt. (d) Relationship between number of pollen particles removed and number of swipes. The solid line inside the shaded area represents the average number of particles removed for each bee. The lower and upper limits of the shaded area represent the standard error. The dashed line represents the prediction from equation (2). The inset shows a semi-log plot of the average number of particles removed.

the translational and rotational kinematics of the basitarsus are determined using an open source tracking software (Tracker by Douglas Brown).

2.4. Observation of pollen removal performance with a honey bee robotic leg

Controlled grooming experiments with a honey bee robotic leg are designed to show the importance of hair-hair interactions during grooming of the compound eyes in honey bees. Because of the constant rotational velocity of the basitarsal pollen brush on the foreleg ($N = 2$), a servomotor is used to replicate the cleaning motion across the eye surface. A non-desiccated honey bee basitarsus is mounted to the leg of the servomotor and the cleaning kinematics simulated in controlled experiments. In figure 2(b), we show a picture of the experimental setup. We use an optical microscope (Olympus SZX16) with a digital camera (Olympus DP72) to accurately control the distance between the surfaces of the eye and basitarsus, which is kept at 250 ± 50 μm.

As shown in figure 2(c), the ablated leg is attached to the arm of a servomotor and a freshly deceased,

nondesiccated honey bee is tethered to a rigid mount. The leg and bee are placed beneath the dissecting microscope on $x-y-z$ stages. We test hairy and smooth, hairless legs. A honey bee leg is made smooth by coating it with a thin layer of wax. The wax covers the hairs and creates a smooth surface, as shown in figure 6(d). A digital camera (Canon EOS 1D) with a macro lens (Canon MP-E 65 mm) is used to take a picture of the pollen-covered honey bee eye before and after it is swiped by the basitarsus. The bee eye is covered with the commercial pollen since it provides dense coverage, as shown in figure 3(c).

We use the MATLAB image analysis toolbox to determine the amount of pollen removed. The contrast between the yellow pollen and black eye surface allows us to isolate and count the pollen by converting the images to black and white. With each leg ($N = 3$) we swipe the eye five times, taking a picture before and after each swipe. The leg is cleaned between each swipe with a can of compressed air (Office Depot Cleaning Duster), to mimic the grooming routines normally employed by honey bees. Before cleaning its eyes, antennae, and head, a honey bee cleans its foreleg either with other legs or with its mandibles and proboscis.

The compressed air removes the majority of pollen from the leg, but not all. The small amounts that are left on the leg may transfer to the eye during a swipe. Additionally, some small clumps of pollen may break up during a swipe and make it appear like there is more pollen on the eye. These two reasons might explain why we obtain some negative values in figure 6(g), especially for swipes beyond the first.

3. Results

3.1. Observations of honey bee grooming

We procure 16 worker honey bees from a hive in Atlanta, Georgia. Since bees usually groom during flight [3], we observe them tethered dorsally to their abdomens, with their legs free to groom. After the bees are tethered, we dip them in a small bowl filled with either commercial pollen, fresh (non-defatted) pollen, or washed (defatted) pollen. The ensuing grooming process is filmed from both the side and below using high-definition camcorders. Side views enable enumeration of grooming movements; bottom views, enumeration of pollen particles removed. We use a uniform backlight to highlight the silhouettes of individual pollen particles. With these techniques we are able to visualize the entire grooming process, and its effectiveness, over several minutes, focusing primarily on the first two minutes. In total, we film 3 grooming cycles for each of 16 individual bees, with 9 individuals grooming commercial pollen, 4 individuals grooming fresh pollen, and 3 individuals grooming washed pollen.

Supplementary video 2 and figure 1(b) show side views of the bee. From these views we observe that the eyes are completely cleaned after 10–20 swipes of the forelegs and find that, on average, a bee swipes its eyes once every 4.2 ± 2.0 s ($N = 16$). Since pollen removal is a discrete process, from hereon we give cleaning rates in units of swipes.

Supplementary video 1 and figure 1(c) show bottom views of the bee, and the particles removed from the body and legs. Since the image is backlit, pollen particles appear as distinct black dots. During the first 10–20 swipes, the bee primarily grooms its eyes and antennae. The eye is groomed by swipes from the pollen brush on the basitarsal region of the forelegs, shown by the small arrow in figure 1(a). Swipes proceed from dorsal to ventral, with a lateral component. The eye-cleaning motions are performed quickly, each taking only 120 ± 66 ms ($N = 3$). Typical eye-cleaning motions are shown in slow motion in supplementary video 3. Each swipe of the eye leaves the leg with visible pollen attached to it. The pollen is removed by mutually rubbing the legs together, which takes about 4.0 ± 3.3 s ($N = 3$). The pollen then falls onto the glass dish.

3.2. Effect of pollenkitt on grooming performance

Naturally, pollen contains a sticky, viscous fluid on its surface called pollenkitt. We use three different types of pollen grains, commercial, fresh, and washed, to observe the effects of this fluid on the overall grooming performance. Scanning electron micrographs of the pollen are shown in figures 3(a) and (b). From these images we see that the commercial pollen contains other biological material from either the bees or the plants they visit. The fresh dandelion pollen contains a thick layer of pollenkitt. Washing the pollen reveals its spines.

Figure 3(c) shows images of bees immediately after being dunked in the commercial, fresh, and washed pollen, respectively. From these images, we see that commercial pollen completely covers the bees, while barely any washed pollen sticks to the bees. Quantitatively, a bee dunked in commercial pollen accumulates 1.9 ± 0.5 mg ($N = 3$), in fresh pollen 1.0 ± 0.2 mg ($N = 3$), and in washed pollen 0.5 ± 0.1 mg ($N = 3$).

From the results in figure 3(d), we can see how the presence of pollenkitt affects the number of pollen particles that are removed and fall to the glass dish below. The rate of pollen removal is constant for the first 5 swipes for the three types of pollen. For the commercial pollen the rate is 430 ± 7.5 pollen particles per swipe, with $R^2 = 0.989$. For the fresh pollen the rate is 139 ± 4.1 pollen particles per swipe, with $R^2 = 0.977$. For the washed pollen the rate is 26.0 ± 3.9 pollen particles per swipe, with $R^2 = 0.259$. After the first 5 swipes, the pollen removal rate drops substantially. For the commercial pollen the rate is 180 ± 3.4 pollen particles per swipe, with $R^2 = 0.985$. For the fresh pollen the rate is 7.8 ± 0.6 pollen particles per swipe, with $R^2 = 0.800$. For the washed pollen the rate is 1.8 ± 0.3 pollen particles per swipe, with $R^2 = 0.567$. For these the plus/minus values represent the 95% confidence interval for the best linear fits. The R^2 values are based on the best linear fits for the average values obtained, or the solid lines in figure 3(d).

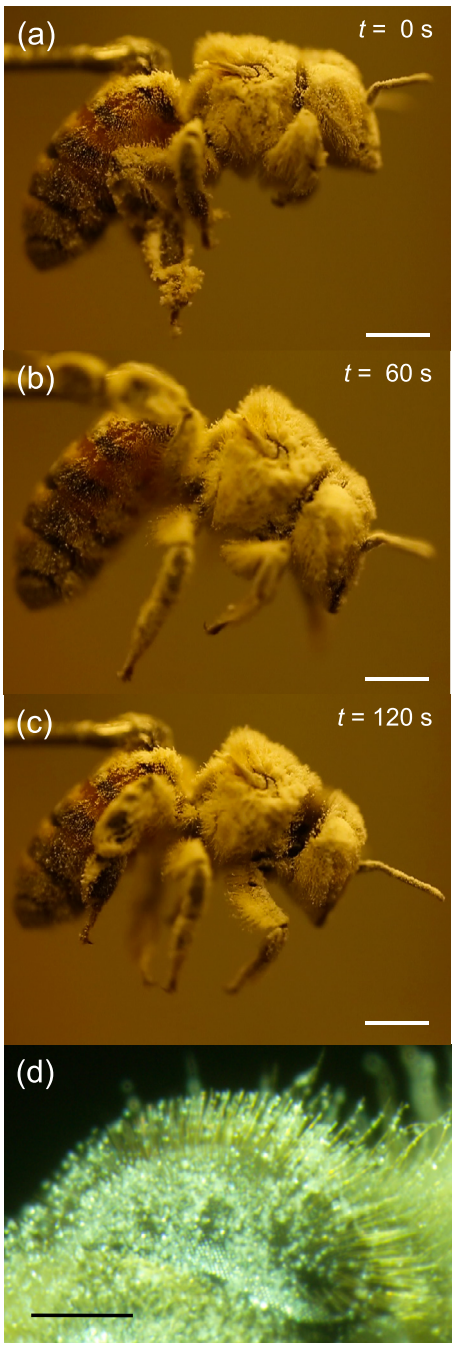

Figure 4. Honey bees cannot clean corn starch. ((a)–(c)) Time lapse of a honey bee grooming while covered in corn starch. (d) The compound eye of a honey bee with corn starch particles. Scale bars represent ((a)–(c)) 1 mm and (d) 0.5 mm.

3.3. Effect of particle size on grooming performance

We perform experiments ($N = 9$) with both commercial pollen of diameter d of 30 μm and corn starch, of 10 μm. A honey bee grooming commercial pollen is shown in figure 1(b) and supplementary video 1, while a honey bee grooming cornstarch is shown in figures 4(a)–(c) and supplementary video 4. We see that a honey bee is completely clean of commercial pollen after 2 min, but is still completely covered in corn starch after the same amount of time grooming.

Pollen is suspended near the tips of the ocular hairs, as shown in the inset of figure 1(a). This suspending ability of the hairs is characterized by the dimensionless group d/S_1, where S_1 is the ocular hair center-to-center spacing. For pollen, $d/S_1 = 0.43$ and for corn starch, $d/S_1 = 0.14$. An ideal spacing is $d/S_1 \approx 1$, which would allow particles to be squeezed by the ocular hairs and remain on the outskirts of the eye. Corn starch falls deep within the pockets created by the ocular hairs, as shown in figure 4(d), making it more difficult to remove.

3.4. Effect of bristle geometry on grooming performance

For effective cleaning, the appendage and ocular hairs should have geometrical properties to promote particle transfer. We denote the cleaner with 0 and the surface to be cleaned with 1, as shown in figure 5(a). For the appendages to clean the eye deeply, the leg hairs should be the same length or longer than the ocular hairs, or $L_1/L_0 \leqslant 1$. The transfer of particles from eye to appendage occurs if the attachment force to the grooming leg is greater than to the eye. This is accomplished when the hair spacing S_0 on the leg is less than the hair spacing S_1 on the eye , or $S_1/S_0 > 1$. Closer spacing of hairs on the leg enables particles to be in contact with more hairs than on the eye, leading to larger contact forces and particle removal. We hypothesize the ratios

$$L_1/L_0 \leqslant 1, \qquad S_1/S_0 > 1 \tag{1}$$

provide two constraints for effective cleaning. We test these hypotheses using measured geometries for 10 insects, like those shown in Figure 5(a), spanning 3 orders.

Figure 5(b) shows the relationship between ratios of hair length L_1/L_0 and spacing S_1/S_0. The insect ocular hairs are generally shorter than the hairs on the leg, shown by the average L_1/L_0 of 0.3. The average spacing ratio S_1/S_0 is 1.7 for insects, indicating that ocular hairs are generally spaced farther than the cleaning hairs.

We have established the proper geometry of hairs for pollen and particle transfer. We proceed with calculating the number of swipes N_{swipe} to clean a honey bee's eye. The geometrical parameters we use in our calculations and their values are tabulated in table 1. Geometrically, the bee eye is an ellipsoid with a surface area $A_1 = 2.5\,\text{mm}^2$ [26]. As shown in figure 6(b), we assume it is hemispherical with effective radius R_1 such that $R_1 = \sqrt{\frac{A_1}{2\pi}} = 0.63$ mm. We find that the spacing S_1 between ocular hairs is 70 μm. Assuming a square lattice yields a hair density $\eta_1 = \frac{1}{S_1^2} = 204$ hairs per mm^2. The total number of hairs N_1 on the eye is $N_1 = \eta_1 A_1 = 510$ hairs. For the worst case scenario when the eye is fully packed with particles, the volume they can occupy is represented by the spherical shell between the eye surface and

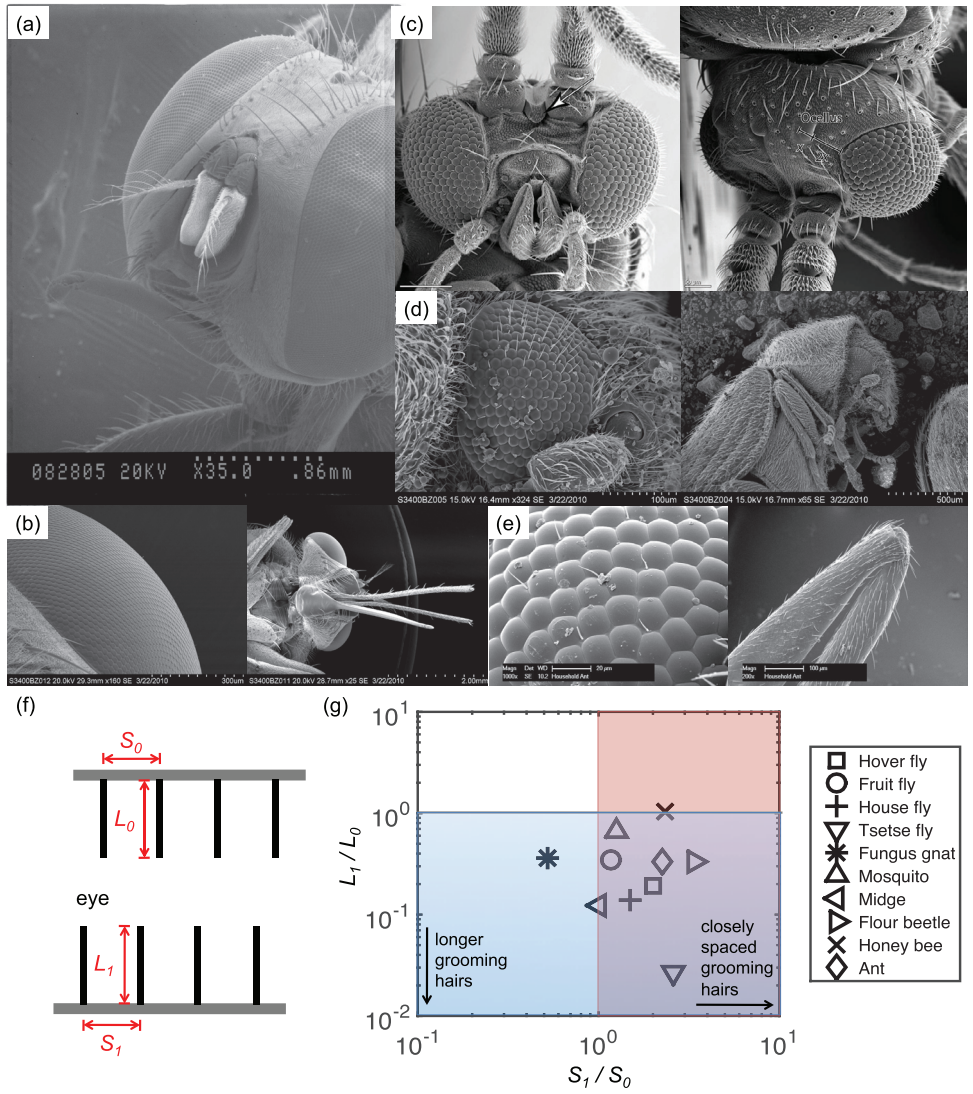

Figure 5. Bristle geometry for insect grooming. (a) house fly (credit: Gregory Paulson. Reproduced with permission from http://webspace. ship.edu/gspaul/)[20], (b) tsetse fly (Reproduced with permission from Barry Martin, Bioimaging Unit, Oxford Brookes University) [21], (c) fungus gnat (Reproduced from http://www.cdfa.ca.gov/plant/ppd/Lucid/Novakia/key/Novakia/Media/Html/N_miloi.htm. Image stated to be in the public domain.) [22], (d) flour beetle (Reproduced with permission from Barry Martin, Bioimaging Unit, Oxford Brookes University) [21], (e) ant (Reproduced with permission from Eugene Choo http://euchoo.net/blog.bk/Boliaology-Part01) [25]. (f) Schematic showing bristle length L_i and spacing S_i, where $i = 0$ for the insect leg and $i = 1$ for the insect eye. (g) Relationship between the hair length ratio L_1/L_0 and hair spacing ratio S_1/S_0 for insects. The data is tabulated in table S1.

hair tips, or $V_1 = \frac{2\pi}{3}[(R_1 + L_1)^3 - R_1^3] - \frac{\pi}{4}d_1^2 L_1 N_1 = 0.90$ mm^3, where the volume occupied by hair has been subtracted. We use a hair length and diameter of $L_1 = 250\ \mu$m and $d_1 = 5\ \mu$m, respectively.

To groom its eye, a honey bee uses its pollen brush near the distal end of its forelegs, or the basitarsal segment. Figure 6(a) shows the pollen brush combing the ocular hairs. We assume the basitarsal segment is a cylinder with a radius $R_0 = 0.15$ mm and length $\lambda_0 = 0.85$ mm, as shown in figure 6(c). The surface area of the basitarsus is simply $A_0 = \pi R_0 \lambda_0 = 0.40$ mm^2, since the pollen brush only resides on half of the basitarsus. The measured hair spacing S_0 is 30 μm, so the hair density assuming a square lattice is $\eta_0 = \frac{1}{S_0^2} = 1100$ hairs mm^{-2}. The hairs are five times more tightly packed on the pollen brush than on the compound eye to ensure adhesion of the particles. The total number of hairs N_0 on the pollen brush of the basitarus is $N_0 = \eta_0 A_0 = 440$ hairs. The volume of the space between the hairs is $V_0 = \frac{\pi}{2}[(R_0 + L_0 \sin\theta)^2 - R_0^2]\lambda_0 - \frac{\pi}{4}d_0^2 L_0 N_0 = 0.074$ mm^3, where $\theta = 35°$ is the angle between the hairs and the leg surface, and $L_0 = 250\ \mu$m and $d_0 = 10\ \mu$m are the length and diameter of the hairs, respectively.

The pollen brush, like a household brush, must collect the pollen that are distributed over the eye surface. Since the eye contains more volume than the leg, eye cleaning requires multiple swipes. In between swipes, the bee brushes off its legs, similar to emptying a dustbin. The number of swipes N_{swipe} required to completely clean a compound eye is given by the ratio of the eye to leg volume,

$$N_{\text{swipe}} = \frac{8[(R_1 + L)^3 - R_1^3] - 3d_1^2 L N_1}{6[(R_0 + L\sin\theta)^2 - R_0^2]L_0 - 3d_0^2 L N_0}. \quad (2)$$

Table 1. Measured values for the bristle geometries of the honey bee eye and grooming leg. Measured from a single worker honey bee.

	Variable	Description	Value	Unit
Leg	L_0	Hair length	250	μm
	S_0	Hair spacing	30	μm
	d_0	Hair diameter	10	μm
	R_0	Leg radius	150	μm
	λ_0	Leg length	850	μm
	η_0	Hair density	1100	hairs mm^{-2}
	θ	Hair tilt angle	35	deg
Eye	L_1	Hair length	260	μm
	S_1	Hair spacing	70	μm
	d_1	Hair diameter	5	μm
	R_1	Eye radius	630	μm
	η_1	Hair density	200	hairs mm^{-2}

Our prediction for number of swipes N_{swipe} is 12, which agrees well with the 10–20 swipes ($N = 9$) observed in experiments, where the bee eye is covered by commercial pollen.

We can also use our model to produce the number of pollen particles removed. In our experiments the honey bees are dunked in commercial pollen just once. We confirm with microscopy that this procedure only accumulates pollen at the tips of their hairs. Therefore, the volume $V_{1,p}$ where pollen collects is only one pollen particle thick. This volume is then found to be: $V_{1,p} = \frac{2\pi}{3}[(R_1 + L_1)^3 - (R_1 + L_1 - d)^3] - \frac{\pi}{4}d_1^2 d N_1 = 0.14$ mm^3, where $d = 30$ μm is the diameter of the pollen particles. Assuming a very loose random packing density $\phi = 0.56$ [27], the total number of pollen particles accumulated on the eye is $N_{\text{pollen}} = \frac{\phi V_{1,p}}{\frac{\pi}{6}d^3} = 5500$. From our model in equation (2), it would take 12 swipes to remove 5500 particles. This total number of particles is comparable with our experimental observations of 3900 ± 2400 particles ($N = 9$) for commercial pollen, as shown in figure 3(d). We can also obtain the rate of removal of pollen particles, or $\frac{N_{\text{pollen}}}{N_{\text{swipe}}} = \frac{5500}{12} = 460$ pollen particles per swipe. This value agrees well with our observed rate for the commercial pollen, or 430 pollen particles per swipe.

3.5. Importance of bristles in grooming performance

To confirm the importance of the leg hairs reaching into the eye, we perform experiments with hairless legs. We design a honey bee robotic leg that uses a severed bee leg to groom the eye of a freshly dead, non-dessicated, honey bee. We use high speed videography to track the motions of a painted basitarsal segment of the foreleg of a grooming bee as it swipes across the eye and find that a rotating servomotor can be used to replicate these motions. The angular velocity of the servomotor is set to match those observed in experiments, or 180 degrees per second ($N = 2$). We conduct experiments with a hairy bee leg and one dipped in wax, which creates a smooth leg, as shown in figure 6(d).

We perform five consecutive brushes, cleaning the leg between swipes with pressurized air. A time sequence of the eye for the first two swipes is shown in figures 6(e) and (f). Figure 6(g) shows the number of pollen particles removed by each of the five swipes. The hairy leg removes four times more pollen than the smooth leg. Most of the pollen is removed in the first swipe, with negligible amounts in additional swipes. This result suggests the bee needs to swipe each location of the eye only once. The smooth leg is an ineffective cleaner, even when using multiple swipes.

Why is the hairy leg able to remove four times as much pollen? Considering our physical picture of hairs providing pockets for particles to accumulate, we compare the volume available for particles on smooth and hairy legs. We define the pollen capacity ratio, comparing hairy to smooth legs, as $\Pi = \frac{V_0}{V_0'}$, where V_0 and V_0' are the volumes available for pollen to accumulate in for a hairy and smooth leg, respectively.

The volume V_0 available for accumulating pollen on a hairy leg is simply the space between the hairs of the pollen, as used in equation (2). This volume may be expressed as $V_0 = \frac{\pi}{2}[(R_0 + L_0 \sin\theta)^2 - R_0^2]\lambda_0 - \frac{\pi}{4}d_0^2 L_0 N_0 = 0.074$ mm^3. When the leg is covered in wax, the radius of the leg is increased by the height of the hairs perpendicular to the leg surface, or $L_0 \sin\theta$, where $\theta = 35°$ is the angle between the leg surface and hair, as shown by figure 6(c). Since a smooth leg only has a surface for pollen to accumulate on, the volume is expressed as the area of the waxed leg times the diameter d of the pollen, or $V_0' = \pi\lambda_0(R_0 + L_0 \sin\theta)d = 0.023$ mm^3. We may then calculate the pollen capacity ratio, the ratio of the storage abilities of the hairy and smooth leg, as

$$\Pi = \frac{2[(R_0 + L_0 \sin\theta)^2 - R_0^2]\lambda_0 - d_0^2 L_0 N_0}{4\lambda_0(R_0 + L_0 \sin\theta)d}. \quad (3)$$

The value of $\Pi = 3.2$ agrees closely with the experimentally observed advantage of 4. We conclude that a hairy leg removes more pollen for two reasons. It has more volume available for the pollen to accumulate in and it can effectively comb through the ocular hairs.

4. Discussion

4.1. Pollenkitt and biological matter promote adhesion

Previous researchers have measured the adhesion of pollen with and without pollenkitt [16]. They found that pollenkitt on dandelion pollen enhances adhesive force to various substrates by a factor of 5. This enhancement was attributed to the pollenkitt and the capillary bridges it may form between the pollen and substrate during adhesion.

In our study, we observe similar effects. As shown in figure 3(c), washed pollen does not stick to the

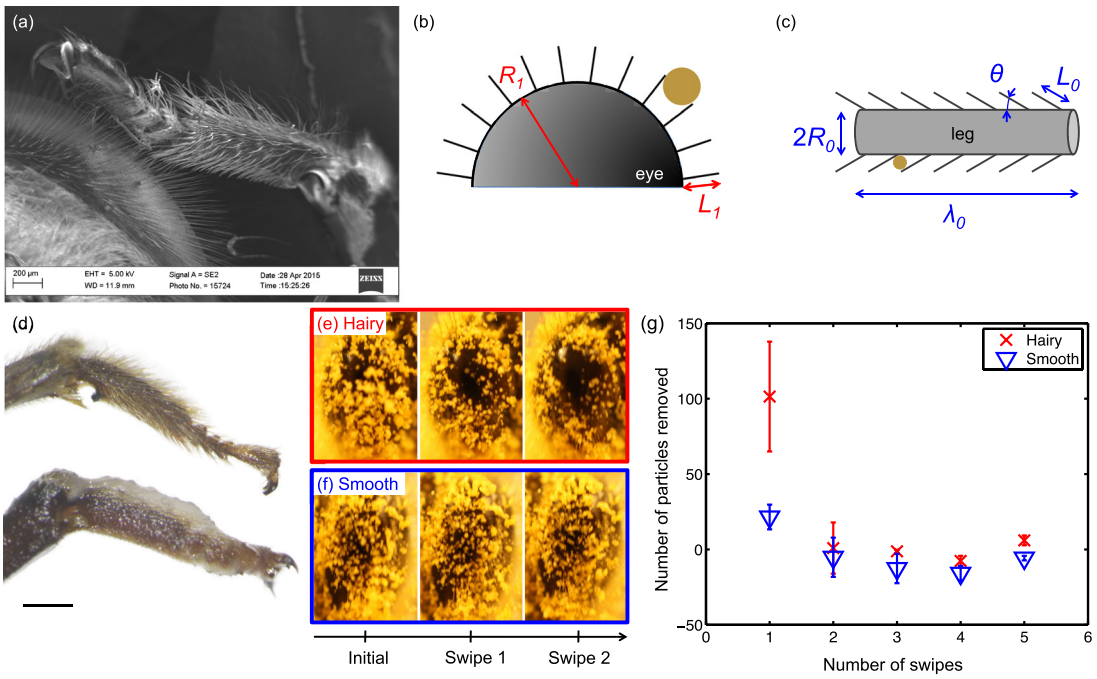

Figure 6. Leg hairs brush ocular hairs. (a) Scanning electron microscope (SEM) image of a honey bee foreleg interacting with the compound eye. Schematics of the (b) eye and (c) foreleg of a honey bee. (d) Picture showing a hairy leg (top) and a smooth, hairless leg (bottom). Scale bar represents 500 μm. ((e)–(f)) Pictures of the honey bee eye before and after two foreleg swipes using a (e) hairy and (f) smooth leg. (g) Relationship between the number of pollen particles removed and number of swipes from a hairy leg (red) and smooth leg (blue). Error bars represent standard error.

honey bees. The bees dunked in washed pollen only accumulated 0.5 mg of pollen, while those dunked in fresh pollen accumulated 1.0 mg of pollen. Our bees accumulated 2 times less pollen when the pollenkitt was removed. Because the bees accumulate less of the washed pollen, the pollen removal rate is affected, as shown in figure 3(d). The initial pollen removal rate for washed pollen was found to be 5 times less than that of fresh pollen. This reduced rate is because there is less pollen to be removed.

On the other hand, the commercial pollen used contains other biological matter, like digested nectar [17], since it is collected from pollen traps in bee hives. When the bees were dunked in the commercial pollen, they accumulated 1.9 mg of pollen. We may therefore assume that the commercial pollen is stickier to the bees, as confirmed visually in figure 3(c). The pollen removal rate for commercial pollen was found to be 3 times larger than that of fresh pollen, which may be attributed to the increased amount of accumulated pollen.

These results lead us to believe that honey bee grooming may be stereotypic, or that the grooming routine remains unchanged when a bee is covered in pollen. The differences in the pollen removal rates can be explained by the changes in initial conditions, or, simply, bees remove more pollen faster if they are initially covered with more.

Further evidence was found when observing the grooming behavior directly. From videos like supplementary video 2, we find the average time between swipes for each bee. For bees grooming commercial pollen, the time between swipes was 3.2 ± 1.2 ($N = 9$). For bees grooming fresh pollen, the time between swipes was 5.8 ± 2.9 ($N = 4$). And for bees grooming washed pollen, the time between swipes was 4.8 ± 0.3 ($N = 3$). When comparing these times using 2-tailed t-tests, we find that their differences are not statistically different. Therefore, swipe frequency is unaffected by initial pollen quantity or the stickiness of the pollen. This claim should be further investigated by extending the observations to more pollen types.

4.2. Particle size relative to hair geometry dictates particle accumulation and transfer

Grain size has a strong effect on whether pollen can be removed. We find that bees can clean themselves easily of commercial pollen within three minutes, removing over 15 000 particles. However, negligible progress is made with corn starch over the same duration, as shown in figures 4(a)–(c). Why is pollen easier to clean than corn starch?

The ability for particles to be suspended by hair is dictated by the ratio of pollen diameter to hair spacing, or d/S_1. For pollen, this ratio is closer to an ideal value of unity, while for cornstarch it is much smaller. The suspension of pollen by the hairs is shown in the inset of figure 1(a), while the penetration of cornstarch within the hair array is shown in figure 4(d). This observation is similar to what has been observed for natural [28] and synthetic [29] fibrillar adhesives that cannot self-clean when soiled by particles smaller than a certain size.

Pollen is easily grabbed by the bee's leg. Grabbing is facilitated if the particles can be wedged within the leg hairs, which requires particle size to be comparable to leg hair spacing, $d \approx S_0$. Particles wedged between leg

hairs experience greater contact area and force. Honey bee legs are well posed to remove and collect pollen from the body because their leg hairs are close together, with a spacing of only $S_0 = 30 \pm 4.4\,\mu$m ($N = 3$). Thus, the grains are effectively wedged between the leg hairs. However, corn starch has a diameter of one-third of the hair spacing, and so it is too small to be wedged. Our observations provide further evidence that the morphology of bees, and their hair, is dictated by the pollen grains they collect, as suggested by previous workers [30].

4.3. Relative hair geometry between legs and eyes dictates combing efficiency

Because the pollen brush on the basitarsal segment of the leg is used to comb through ocular hairs during grooming, their relative hair geometries play a critical role in cleaning efficiency. The inequalities in equation (1) provide the geometrical constrains for effective particle transfer. The blue and red rectangles in figure 5(b) represent the regimes in equation (1). Only one insect species, the fungus gnat, does not meet these requirements.

At at the length scale of humans, the complete and effective removal of particulates may not be critical. However, for insects, particle adhesion can have detrimental effects. The importance of cleanliness is evident when observing the time and effort employed by bees, flies, and other insects during grooming. The size of accumulated debris is on the order of the size of their sensory and locomotor structures, and so their removal is critical for survival. Insects may motivate technological designs for effective cleaning at the microscale, especially with the emergence and growth of microelectromechanical systems (MEMS) [31].

5. Conclusion

In this study, we outlined the principles of cleaning by pollinating insects. An important trait of insects that makes cleaning possible is their hairiness. Cleaning is facilitated by having hairs on both the surface to be cleaned and the cleaner. The geometry of the hair arrays on both surfaces dictate their efficiency. As has been previously suggested, hair spacing on the body is tuned to the particles they collect to facilitate particle suspension for easy removal, while hair spacing on the grooming legs enables the effective transfer of particles from the body to the legs and determines the amount of pollen removed during each swipe. Additionally, we find that grooming behavior is unaffected by pollen type or initial pollen accumulation. However, the presence of pollenkitt, or the viscous fluid on the surface of pollen, plays an important role in pollen accumulation. Honey bees accumulated half as many pollen grains when the pollenkitt was removed. This study is the first to provide physical insight into the critical process of pollination. The methods used by pollinating insects for accumulating and removing micro-scale particles may motivate designs for cleaning human-made surfaces.

Acknowledgments

We thank F Durand, S Pusulri, and E Jung for their early contributions, Dr Jennifer Leavey and the Georgia Tech Urban Honey Bee Project for providing our bee samples, the Center for Nanoscale Characterization (CNC) supported by the Georgia Tech College of Engineering for providing access to their scanning electron microscope (SEM), and financial support of the NSF (PHY-1255127).

References

[1] Crepet W L, Friis E M, Nixon K C, Lack A J and Jarzembowski E A 1991 Fossil evidence for the evolution of biotic pollination *Phil. Trans. R. Soc.* **333** 187–95
[2] Jander U 1966 Untersuchungen zur stammesgeschichte von putzbewegungen von tracheaten *Z. Tierpsychol.* **23** 799–844
[3] Casteel D B 1912 *The Behavior of the Honey Bee in Pollen Collection* (Alexandria: Library of Alexandria)
[4] Lipps K L 1973 Comparative cleaning behavior in Drosophila *PhD Thesis* University of California, Davis
[5] Hlavac T F 1975 Grooming systems of insects—structure, mechanics *Ann. Entomol. Soc. Am.* **68** 823–6
[6] Szebenyi A L 1969 Cleaning behaviour in Drosophila-melanogaster *Animal Behav.* **17** 641–51
[7] Basibuyuk H H and Quicke D L J 1999 Grooming behaviours in the Hymenoptera (Insecta): potential phylogenetic significance *Zoological J. Linnean Soc.* **125** 349–82
[8] Böröczky K, Wada-Katsumata A, Batchelor D, Zhukovskaya M and Schal C 2013 Insects groom their antennae to enhance olfactory acuity *Proc. Natl Acad. Sci.* **110** 3615–20
[9] Thorp R W 1979 Structural, behavioral, and physiological adaptations of bees (Apoidea) for collecting pollen *Ann. Missouri Botanical Garden* **66** 788–812
[10] Connolly K 1968 The social facilitation of preening behaviour in *Drosophila melanogaster Animal Behav.* **16** 385–91
[11] Valentine B D 1973 Grooming behavior in Coleoptera *Coleopterists' Bull.* **27** 63–73
[12] Seeds A M, Ravbar P, Chung P, Hampel S, Midgley F M, Mensh B D and Simpson J H 2014 A suppression hierarchy among competing motor programs drives sequential grooming in Drosophila *eLife* **3** e02951
[13] Hackmann A, Delacave H, Robinson A, Labonte D and Federle W 2015 Functional morphology and efficiency of the antenna cleaner in Camponotus rufifemur ants *R. Soc. Open Sci.* **2** 150129
[14] Winston M L 1991 *The Biology of the Honey Bee* (Cambridge: Harvard University Press)
[15] Pasteels J J and Pasteels J M 1972 *Les Soies Cuticulaires des Megachilidae (Hymenoptera Apoidea) vues au Microscope électronique à Balayage* (Bruxelles: Palais des Académies)
[16] Lin H, Gomez I and Meredith J C 2013 Pollenkitt wetting mechanism enables species-specific tunable pollen adhesion *Langmuir* **29** 3012–23
[17] Nogueira C, Iglesias A, Feás X and Estevinho L M 2012 Commercial bee pollen with different geographical origins: a comprehensive approach *Int. J. Mol. Sci.* **13** 11173–87
[18] Pacini E and Hesse M 2005 Pollenkitt–its composition, forms and functions *Flora-Morphol. Distrib. Funct. Ecol. Plants* **200** 399–415
[19] Carlson S D and Chi C 1974 Surface fine structure of the eye of the housefly (musca domestica): ommatidia and lamina ganglionaris *Cell Tissue Res.* **149** 21–41
[20] Paulson G S 2000 Scanning electron micrographs of insects and other arthropods http://webspace.ship.edu/gspaul/
[21] Osterrieder A 2012 Of flour beetle grannies and cuddly head lice—taking a closer look at creepy crawlers http://plantcellbiology.com/2012/02/

[22] California Department of Food and Agriculture 2007 California Department of Food and Agriculture Novakia miloi Kerr www.cdfa.ca.gov/plant/ppd/Lucid/Novakia/key/Novakia/Media/Html/N miloi.htm
[23] Gregory D and Marshall D 2015 Scanning electron micrograph of midge eye, showing individual ocelli (facets) http://wellcomeimages.org/indexplus/image/B0000664.html
[24] Alexandre-Pires G, Ramilo D, Diaz S, Meireles J, Boinas F and Pereira da Fonseca I 2010 Investigating morphological structures of culicoides from obsoletus complex by using scanning electron microscopy and composed optical microscopy *Microscopy: Science, Technology, Applications and Education* (Badajoz: Formatex Research Center) pp 792–802
[25] Choo E 2008 Boliaology Part 01 http://euchoo.net/blog.bk/Boliaology-Part01
[26] Streinzer M, Brockmann A, Nagaraja N and Spaethe J 2013 Sex and caste-specific variation in compound eye morphology of five honeybee species *PloS One* **8** e57702
[27] Dullien F A L 2012 *Porous Media: Fluid Transport and Pore Structure* (New York: Academic)
[28] Hosoda N and Gorb S N 2010 Friction force reduction triggers feet grooming behaviour in beetles *Proc. R. Soc.* B **278** rspb20101772
[29] Menguc Y, Rohrig M, Abusomwan U, Holscher H and Sitti M 2014 Staying sticky: contact self-cleaning of gecko-inspired adhesives *J. R. Soc. Interface* **11** 20131205
[30] Roberts R B and Vallespir S R 1978 Specialization of hairs bearing pollen and oil on the legs of bees (Apoidea: Hymenoptera) *Ann. Entomol. Soc. Am.* **71** 619–27
[31] Gad-el Hak M 2001 *The MEMS Handbook* (Boca Raton, FL: CRC Press)